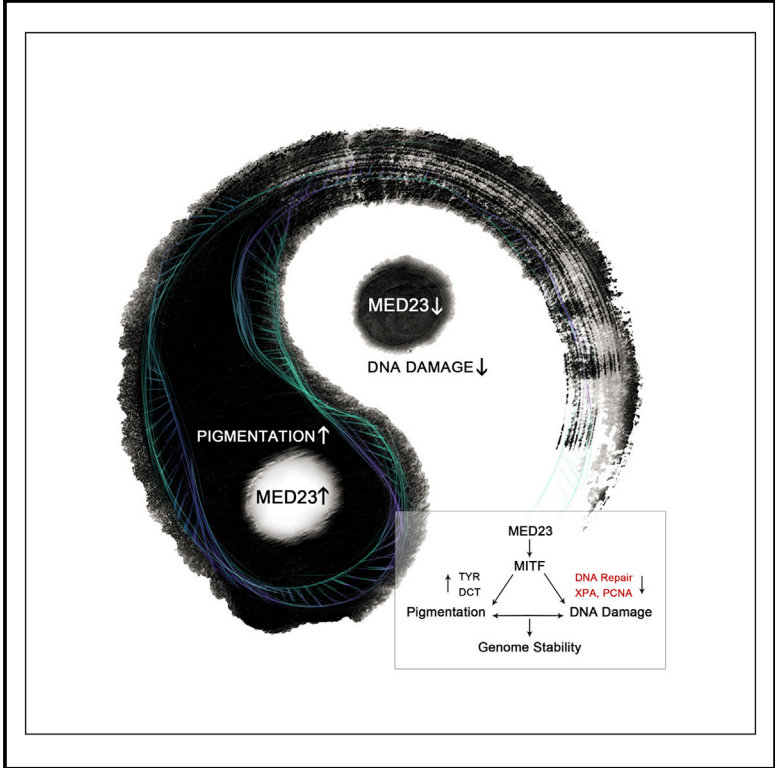


Mediator MED23 Links Pigmentation and DNA Repair through the Transcription Factor MITF

Graphical Abstract



Authors

Min Xia, Kun Chen, Xiao Yao, ..., Jun Yan, Zhen Shao, Gang Wang

Correspondence

gwang@sibcb.ac.cn

In Brief

Xia et al. find that MED23 controls *Mitf* expression by modulating its enhancer function, thus connecting DNA repair to pigmentation.

Highlights

- Mediator MED23 regulates pigmentation in cells and in zebrafish
- *Med23* deficiency facilitates DNA repair and prevents UV-induced DNA damage
- MED23/MITF axis is critical in coupling pigmentation and DNA repair
- MED23 controls *Mitf* expression by modulating its enhancer function

Accession Numbers

GSE98607
GSE98606



Mediator MED23 Links Pigmentation and DNA Repair through the Transcription Factor MITF

Min Xia,^{1,4} Kun Chen,^{1,2,4} Xiao Yao,¹ Yichi Xu,³ Jiaying Yao,³ Jun Yan,³ Zhen Shao,³ and Gang Wang^{1,2,5,*}

¹State Key Laboratory of Cell Biology, CAS Center for Excellence in Molecular Cell Science, Shanghai Institute of Biochemistry and Cell Biology, Chinese Academy of Sciences, University of Chinese Academy of Sciences, 320 Yueyang Road, Shanghai 200031, China

²School of Life Science and Technology, ShanghaiTech University, 100 Haik Road, Shanghai 201210, China

³CAS-MPG Partner Institute for Computational Biology, Shanghai Institute for Biological Sciences, Chinese Academy of Sciences, Shanghai 200031, China

⁴These authors contributed equally

⁵Lead Contact

*Correspondence: gwang@sibcb.ac.cn

<http://dx.doi.org/10.1016/j.celrep.2017.07.056>

SUMMARY

DNA repair is related to many physiological and pathological processes, including pigmentation. Little is known about the role of the transcriptional cofactor Mediator complex in DNA repair and pigmentation. Here, we demonstrate that Mediator MED23 plays an important role in coupling UV-induced DNA repair to pigmentation. The loss of *Med23* specifically impairs the pigmentation process in melanocyte-lineage cells and in zebrafish. *Med23* deficiency leads to enhanced nucleotide excision repair (NER) and less DNA damage following UV radiation because of the enhanced expression and recruitment of NER factors to chromatin for genomic stability. Integrative analyses of melanoma cells reveal that MED23 controls the expression of a melanocyte master regulator, *Mitf*, by modulating its distal enhancer activity, leading to opposing effects on pigmentation and DNA repair. Collectively, the Mediator MED23/MITF axis connects DNA repair to pigmentation, thus providing molecular insights into the DNA damage response and skin-related diseases.

INTRODUCTION

Degree of pigmentation is responsible for skin color and tanning, and it is a useful predictor of skin cancer in humans (Garibyan and Fisher, 2010; Lin and Fisher, 2007). Pigmentation in animals is determined by the number, size, and cellular distribution of melanosomes, which are subcellular compartments comprised of melanocytes. Epidermal melanocytes can respond to UV radiation (UVR) by inducing the synthesis of melanin in melanosomes and transferring melanin to surrounding keratinocytes, also known as the tanning response. In addition, melanin also plays a prominent role in providing protection against UV-induced DNA damage, which can transform melanocytes into malignant melanoma, an aggressive form of skin cancer, as well as in the development of xeroderma pigmentosum (XP). Maintaining the genomic stability of melanocytes is pivotal for the prevention of

malignant melanoma, whereas DNA repair is most essential for protection against carcinogenesis (Budden and Bowden, 2013; Karahail et al., 2012). UVR generates mutagenic photolesions, generally cyclobutane pyrimidine dimers (CPDs) and 6-4 photo-products (6-4PPs), which are primarily removed through the nuclear excision repair (NER) pathway. NER corrects UV-induced DNA damage and chemically induced bulky lesions via a multistep process involving numerous repair factors, including ERCC1, ERCC3, ERCC4, XPA, XPC, XPG, DDB2, and PCNA (DiGiovanna and Kraemer, 2012; Lehmann et al., 2011). The importance of the NER pathway has been demonstrated by studying XP, trichothiodystrophy (TTD), and Cockayne syndrome (CS) patients who have lost one of these NER proteins and are incapable of repairing UV-induced DNA lesions, rendering them predisposed toward UV-related skin cancers (Kraemer et al., 2007; Lehmann et al., 2011). Pigmentation and DNA repair factors are transcriptionally regulated by numerous protein complexes and signaling pathways. For example, the homeostasis of pigmentation is notably modulated by the basic helix-loop-helix leucine zipper (bHLHZip) transcription factor MITF, which is a master regulator of melanocyte specification (Steingrímsson et al., 2004). NER factors are also tightly controlled by temporarily regulated gene expression (Compe and Egly, 2012; Hanawalt and Spivak, 2008). However, as a vital component of general transcription cascades, the role of the Mediator complex in both processes remains unclear.

The Mediator complex is an evolutionarily conserved, multiprotein coactivator that connects transcription factors to the RNA polymerase II (Pol II) machinery (Malik and Roeder, 2010; Yin and Wang, 2014). Considering the specific interactions between transcription factors and different Mediator subunits, the Mediator complex could serve as an integrative hub linking multiple pathways responsible for diverse biological processes, such as the nuclear hormone receptor pathway (via MED1) (Kang et al., 2002), Wnt signaling pathway (via MED12) (Kim et al., 2006), and mitogen-activated protein kinase (MAPK) signaling pathway (via MED23) (Stevens et al., 2002; Wang et al., 2009). In an effort to investigate the role of MED23 in melanoma cells, we uncovered a function for the Mediator complex in pigmentation and the DNA damage response. Specifically, *Med23* deficiency dramatically impairs the pigmentation process while enhancing UV-induced NER, which is seemingly controlled through the melanocyte master transcription factor MITF. These findings demonstrate a

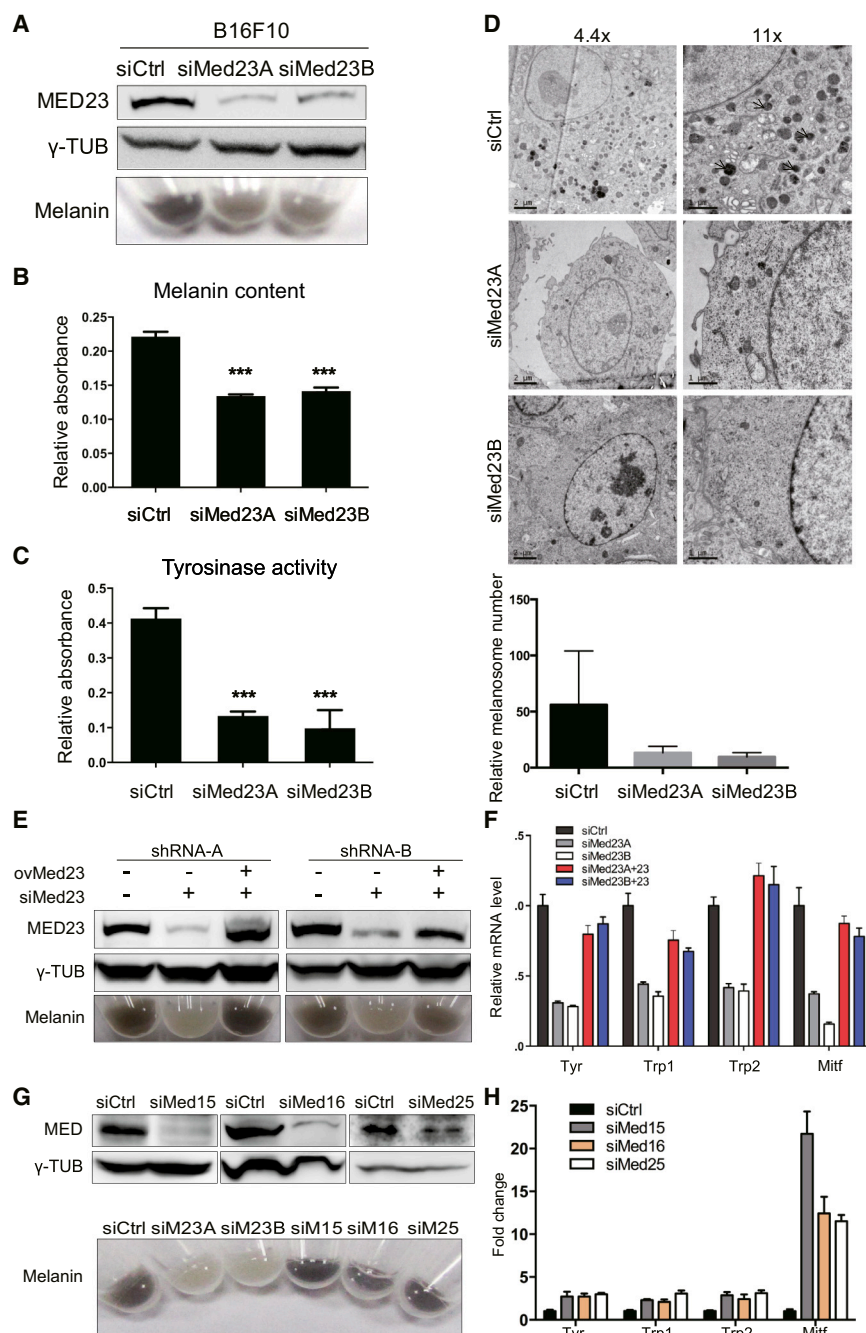


Figure 1. Loss of *Med23* Inhibits the Pigmentation Process

(A) Characteristics of control and si*Med23* B16F10 cells. siMed23A and siMed23B indicated two distinct shRNA sequences that target *Med23*. γ-TUBULIN was blotted as internal control. Bottom: siCtrl and si*Med23* cell pellets in tubes.

(B) Melanin content of control and si*Med23* melanoma cells. Levels of melanin were determined by measuring the absorbance at 405 nm. ****p* < 0.001; error bars indicate SEM.

(C) Tyrosinase activity measured by L-DOPA oxidation using lysates from control and si*Med23* melanoma cells. The data show mean ± SEM of three experiments. ****p* < 0.001.

(D) Transmission electron microscopy (TEM) images of control (top) and si*Med23* (center and bottom) melanoma cells at different magnifications. Arrows indicate melanosomes in the cytoplasm. Also shown is quantitation of the TEM images. Error bars indicate SEM.

(E) Rescue experiment with human *MED23* in si*Med23* cells. si*Med23* cells were infected with retroviruses expressing h*MED23* (ov*MED23*) and selected with hygromycin. Total protein extracts were analyzed by western blot using the indicated antibodies, with γ-TUBULIN as an internal control. Bottom: cell pellets of control, si*Med23*, and h*MED23* rescued cells.

(F) Quantitative RT-PCR analysis of multiple pigmentation-related genes. The expression was normalized to *Gapdh*. Error bars indicate SEM.

(G) Knockdown efficiency of multiple Mediator subunits (*Med15/Med16/Med25*) in B16F10 cells. Bottom: control and si*Med* cell pellets.

(H) qRT-PCR analysis of pigmentation-related genes following Mediator subunit knockdown. The expression was normalized to *Gapdh*. Error bars indicate SEM.

distinct role for Mediator MED23 in regulating pigmentation and DNA damage repair, providing a mechanistic link between pigmentation- and DNA repair-related diseases.

RESULTS

Mediator MED23 Specifically Regulates Pigmentation In Vitro

In an effort to expand our previous investigation into the role of MED23 in cancer (Yang et al., 2012), we examined multiple can-

cer types, including a darkly pigmented mouse melanoma cell line, B16F10. Interestingly, when we knocked down *Med23* in B16F10 cells, the darkly pigmented cells adopted a much lighter color (Figure 1A), and the melanin content was significantly decreased (Figure 1B). We then assayed tyrosinase activity, a rate-limiting enzyme in melanogenesis, by quantifying the oxidation of L-3,4-dihydroxyphenylalanine (L-DOPA) in B16F10 cells. Consistently, we found that tyrosinase activity was significantly reduced following *Med23* knockdown (Figure 1C). Ultrastructural studies using transmission electron microscopy (TEM) revealed a drastic decrease in the number of darkly pigmented melanosomes in si*Med23* cells (Figure 1D). We expanded these studies to include additional melanocyte-lineage cells and found that the expression levels of pigmentation-related genes were consistently downregulated following knockdown of *Med23* in Clone M-3 and B16 mouse melanoma cells as well as in primary human melanocytes (Figures

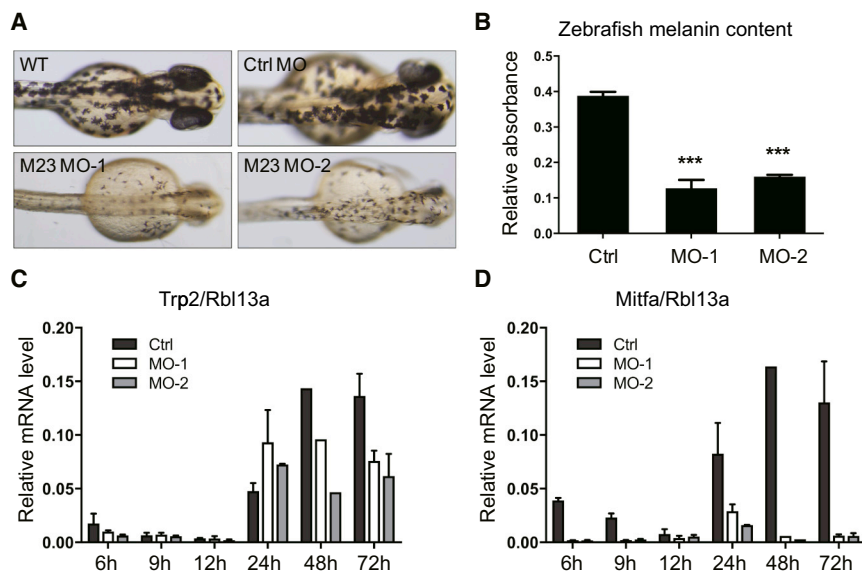


Figure 2. Knocking Down *Med23* Inhibits Pigmentation in Zebrafish

(A) Zebrafish embryos injected with Ctrl MO, *Med23* MO-1, or *Med23* MO-2 were analyzed. The images show dorsal views, with the anterior to the right.

(B) Melanin content of Ctrl MO, *Med23* MO-1, and *Med23* MO-2 embryos. *** $p < 0.001$; error bars indicate SEM.

(C and D) qRT-PCR analysis of the pigmentation-related genes *Trp2* (C) and *Mitf* (D) in zebrafish at the indicated time points. The expression was normalized to *Rbl13a*. Error bars indicate SEM.

S1A–S1C). Next, we compared gene expression levels in immortalized WT and *Med23*^{−/−} mouse embryonic fibroblast (MEF) cells and found a lower basal level of expression for these genes in *Med23*^{−/−} MEFs (Figure S1D). These observations suggest that MED23 may play a role in the pigmentation process.

To exclude possible off-target effects for the *Med23* short hairpin RNA (shRNA) sequences, the human *MED23* gene, which is homogeneous to the mouse *Med23* gene, was reintroduced into the *Med23*-depleted B16F10 line using retrovirus transduction. Ectopic expression of human *MED23* rescued the albinotic color phenotype in *Med23* knockdown B16F10 cells (Figure 1E) as well expression of the pigmentation-related genes, demonstrating that these phenotypes were not due to off-target effects (Figure 1F). Next, we investigated whether MED23 was specific among the Mediator components for the regulation of pigmentation. The Mediator complex is a multi-subunit protein complex, with each component playing a distinct role in different biological functions (Malik and Roeder, 2010). Several Mediator subunits were retrovirally depleted (Figure 1G). However, depletion of other subunits, such as MED15, MED16, and MED25, failed to inhibit expression of the essential pigmentation genes and, in fact, increased the expression of these genes compared with control cells, demonstrating the specificity of MED23 in the pigmentation process (Figure 1H). Taken together, loss of *Med23* specifically inhibits the pigmentation process in melanocyte-lineage cells.

Knocking Down *Med23* in Zebrafish Inhibits Pigmentation

To investigate the *in vivo* function of MED23 in pigmentation, we employed the zebrafish model system, which is a well-established organism for studying melanocyte biology (Kimmel et al., 1995). The zebrafish *MED23* protein sequence exhibits extremely high conservation with the human and mouse *MED23* (Yin et al., 2012; Zhu et al., 2015). Two morpholinos (MOs) were designed to specifically block translation of the

zefrafish *Med23* mRNAs. Pigmentation in *Med23*-MO zebrafish was significantly impaired with respect to melanosome size and number (Figure 2A) as well as whole-body melanin content (Figure 2B). Pigmentation gene expression was quantified at different stages of zebrafish development from 6–72 hours post fertilization (hpf), and these genes showed significantly lower expression at most development stages compared with control fish (Figures 2C and 2D). Considering that MED23 regulates pigmentation in culturing cells, we conclude that MED23 regulates the pigmentation process both *in vitro* and *in vivo*.

Med23 Deficiency Facilitates Nucleotide Excision Repair and Prevents UV-Induced DNA Damage

The skin is primarily reliant on melanocytes for photoprotection, which they mediate by producing melanin (i.e., the pigmentation process) to protect genomic DNA from solar UV-induced damage, thereby reducing the risk of skin cancer (Lin and Fisher, 2007). Considering that MED23 specifically regulates the pigmentation process, we asked whether MED23 also plays a role in UV-induced DNA damage repair. Control and *Med23*-deficient B16F10 cells were used to characterize the activation of DNA damage sensors and their downstream effectors. Upon exposure to UV radiation, the DNA damage sensor phospho-ATR (pATR) showed strong activation that gradually decayed over time; a similar trend was observed for phosphorylated CHK1, which is a downstream effector of pATR (Figure 3A). *Med23* depletion seemed not to change much of the phosphorylation of ATR or CHK1; however, the activation and kinetics of the DNA damage marker γ -H2AX were significantly reduced and delayed in *Med23*-deficient cells (Figure 3A). To determine the spatiotemporal localization of γ -H2AX following UV radiation, control and *Med23*-depleted cells were exposed to UV radiation and then immunostained with an antibody against γ -H2AX. This UV-induced γ -H2AX staining signal gradually increased with time post UV treatment in control cells but was greatly attenuated in *Med23*-deficient cells (Figure 3B). We further verified the effects of MED23 on the DNA damage response using wild-type (WT) and *Med23*^{−/−} MEFs. Using this system, the intensity of γ -H2AX was even more strongly impaired in *Med23*^{−/−} MEF cells compared with WT cells, likely because of the complete depletion of *Med23* (Figure S2). To test whether MED23

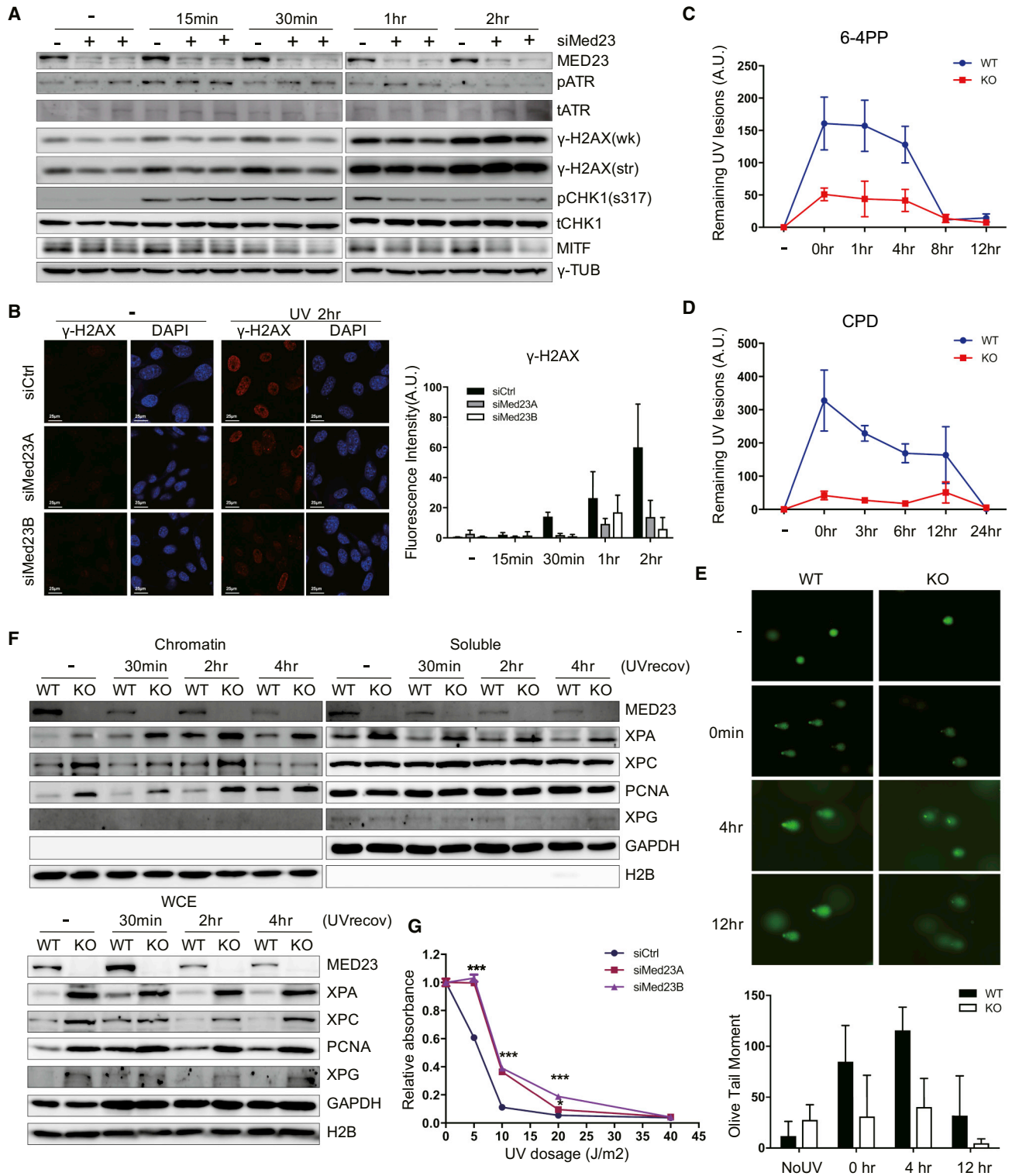


Figure 3. Med23 Deficiency Comprises UV Radiation-Induced DNA Damage

(A) Expression of DNA damage response factors at different time points after UV radiation. B16F10 cells were exposed to 70 J/m² ultraviolet C (UVC). After further incubation for the indicated periods of time, cells were harvested and subjected to immunoblotting analysis of the indicated proteins. wk and str represent weak and strong exposure, respectively. γ -TUBULIN was blotted as an internal control.

(legend continued on next page)

is specifically involved in UV-induced DNA damage and repair, we studied the function of MED23 in DNA double-strand break (DSB) repair induced by ionization radiation (IR). However, we found no significant differences in γ -H2AX levels between WT and *Med23*^{-/-} MEF cells using immunoblotting or immunostaining (Figures S3A and S3B). These results indicate that UV radiation, but not IR-induced DNA damage, is significantly and specifically attenuated by the loss of *Med23*, suggesting a specific role for MED23 in UV-induced DNA damage response and repair pathways.

Because DNA damage was significantly lower in *Med23*-null cells, we anticipated that cells lacking MED23 may show fewer UV-activated photoproducts with enhanced UV-induced DNA repair ability. UV-generated mutagenic DNA photolesions, mostly CPDs and 6-4PPs, can lead to mutations if not repaired, perhaps leading to melanoma or XP diseases (Hodis et al., 2012). Such photolesions are removed through the multistep NER pathway, which involves the repair factors XPA, XPC, and PCNA as well as many others. To study the function of MED23 in the DNA damage response and repair pathways, WT and *Med23*^{-/-} MEF cells were subjected to UV radiation, and UV-generated DNA photolesions were examined. Immunofluorescence measurements using antibodies against CPD and 6-4PP were utilized to evaluate UV-induced photolesions and the damage repair rate. We found that CPD and 6-4PP production levels were largely attenuated immediately following irradiation in *Med23*^{-/-} cells compared with WT MEFs (Figures 3C and 3D). In WT MEF cells, the clearance of 6-4PP and CPD took nearly 12 and 24 hr, respectively. However, in *Med23*^{-/-} MEF cells, these photolesions were barely detectable immediately following UV radiation, and they were maintained at low levels until fully repaired. To verify this result, we analyzed DNA damage in WT and *Med23*^{-/-} MEF cells using an alkaline comet assay. In the absence of UV radiation, comet tail size was not significantly different between WT and *Med23*^{-/-} cells. However, DNA damage was largely increased in WT MEFs compared to that in *Med23*^{-/-} MEF cells immediately upon UV radiation, as indicated by the comet tails (Figure 3E). These observations indicate that the loss of MED23 greatly attenuates UV-induced photolesions, possibly by maintaining genomic DNA in a more stable state.

Because photolesions were less abundant and DNA damage was rapidly attenuated in *Med23*-deficient cells, we investigated

how MED23 affects the NER pathway and DNA repair. We found that MED23 negatively influenced the expression and kinetics of key NER proteins, including nuclear accumulation and recruitment to chromatin after UV radiation. Immunoblotting showed that the expression levels of several NER proteins, including XPA, PCNA, and XPC, were clearly elevated in *Med23*^{-/-} MEFs compared with WT cells (Figure 3F). In the melanotic B16F10 cell line, we observed an increase in XPA expression in sh*Med23* cells (Figure S3E). We performed a chromatin isolation assay and observed that there were more NER proteins bound to chromatin in *Med23*^{-/-} MEF cells, with increased association following UV radiation (Figure 3F). Among the NER factors, XPA showed a strong association with chromatin in *Med23*^{-/-} MEF cells, indicating increased DNA repair ability. We performed the same assays using control and *Med23* knockdown melanoma cells and found that XPA and PCNA levels were consistently elevated in *Med23*-depleted cells with enhanced chromatin association (Figures S3C–S3E). Thus, *Med23* knockdown can enhance NER capacity by boosting the expression of NER factors as well as by promoting their recruitment to chromatin.

MITF Is a Critical Link in Coupling Pigmentation and DNA Repair

To investigate the mechanisms through which MED23 regulates pigmentation and DNA repair, we explored how MED23 controls gene expression in melanoma cells. Using RNA sequencing (RNA-seq) of control and si*Med23* B16F10 cells, we performed a gene ontology (GO) analysis, which revealed that the downregulated transcripts in *Med23* knockdown cells were primarily associated with pigmentation-related processes such as melanin biosynthesis, pigment metabolism, and pigment cell differentiation, consistent with the color changes observed in melanoma cells (Figures 4A and 4B). In addition, a Kyoto Encyclopedia of Genes and Genomes (KEGG) pathway analysis of all downregulated genes identified the melanogenesis pathway as significantly affected, which involves essential pigmentation genes such as *Tyr*, *Mc1r*, and *Trp1*, among others (Figures S4A and S4B). The transcription factor MITF is known to be a master regulator of pigmentation and melanocyte development (Goding, 2000; Strub et al., 2011). Because MITF controls the expression of many genes that are required for melanin synthesis and melanocyte differentiation (Bertolotto et al., 1998), we went

(B) Fluorescent immunostaining of γ -H2AX. Cells were irradiated with 70 J/m² UV light, incubated for different times, and then stained with anti- γ -H2AX (red). DAPI (blue) was used for nuclear counterstaining. Left: representative fluorescent immunostaining images of γ -H2AX. Right: quantification of the immunofluorescence shown on the left. The intensity of nuclear fluorescence was measured using a confocal microscope, and the graphs were processed by Image-Pro Plus. The fluorescence intensity (a.u.) was determined by the overall mean intensity relative to the area. For each sample, at least 100 nuclei were analyzed in three independent experiments; error bars represent SEM.

(C and D) DNA damage was determined by fluorescent immunostaining with antibody against either 6-4PP (C) or CPD (D) at various times after global UV radiation (70 J/m²). At least 100 cells were analyzed per sample. Error bars represent the SEM of three independent experiments.

(E) Comet assay breaks. DNA strand breaks of globally UV-irradiated (40 J/m²) WT and *Med23*^{-/-} MEF cells were analyzed by alkaline comet assay after incubation for the indicated times. Bottom: breaks were quantified as olive tail moment by the CASP software. At least 50 cells were analyzed per sample. Histograms represent mean \pm SEM of three independent experiments.

(F) Chromatin-bound NER factors after UV radiation. Chromatins from UV-irradiated WT and *Med23*^{-/-} MEF cells were isolated after incubation for different times and immunoblotted using antibodies against XPA, XPC, PCNA, and XPG. Histone H2B and GAPDH were loaded as internal controls for chromatin and soluble fractions, respectively.

(G) UV sensitivity of control and *Med23*-deficient melanoma cells. Control and *Med23* knockdown melanoma cells were UV-irradiated, followed by a survival clonal formation assay to analyze UV sensitivity. **p* < 0.05, ****p* < 0.001. Error bars indicate SEM.

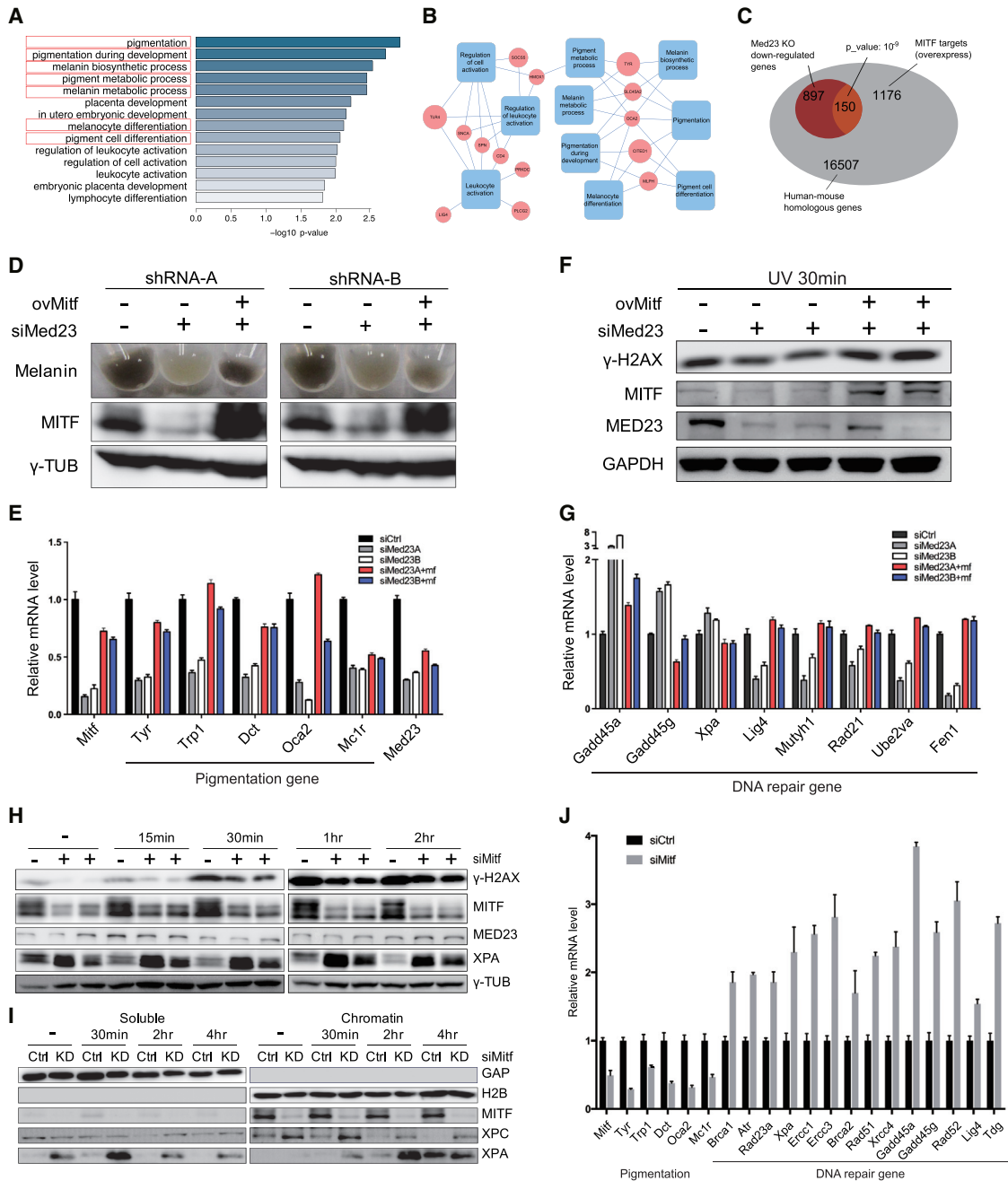


Figure 4. MITF Is a Key Effector for MED23 in Regulating Pigmentation and DNA Repair

(A) GO analysis of the downregulated genes following *Med23* knockdown in B16F10 cells. 190 downregulated genes (fold change ≥ 4) were subjected to DAVID analysis (<http://david.abcc.ncifcrf.gov>). The p value and ontology for each class are indicated.

(B) Gene regulatory network. Blue round rectangles represent biological processing, red circles represent corresponding genes, and the circle size indicates the fold change of downregulated genes.

(C) Venn diagrams showing the intersection of MITF-targeted genes from ChIP-seq and downregulated genes following *Med23* depletion. The number of genes and p values are indicated.

(D) Introducing hMITF in siMed23 melanoma cells. siMed23 cells were infected with retroviruses expressing human MITF and then selected with hygromycin. Top: cell pellets of control, siMed23, and hMITF-expressed siMed23 cells.

(E) qRT-PCR analysis of several pigmentation-related genes in control, siMed23, and hMITF-expressed siMed23 melanoma cells. The expression was normalized to *Gapdh*. Error bars indicate SEM.

(F) Introducing hMITF in siMed23 melanoma cells. Control, siMed23, and stably hMITF-expressed B16F10 cells were exposed to 70 J/m² UVC. After further incubation for 30 min, cells were harvested and subjected to immunoblotting analysis of the indicated proteins. GAPDH was blotted as an internal control.

(legend continued on next page)

on to compare the genes that were downregulated by *Med23* knockdown with 1,326 MITF-targeted genes that were identified previously (Hoek et al., 2008; Strub et al., 2011). Significantly, 150 overlapping genes were identified in these studies ($p = 2.5 \times 10^{-9}$), suggesting that a large number of *Med23*-downregulated genes are transcriptionally targeted by MITF (Figure 4C). We also found that MITF expression itself was downregulated at both the protein and mRNA levels in *Med23* knockdown B16F10 cells (Figures 4D and 4E), and, looking back to the zebrafish experiments, MITF expression was also strongly inhibited in *Med23* morphants (Figures 2C and 2D). Importantly, ectopically introduced *Mitf* redarkened the albinotic color of si*Med23* melanoma cells and completely rescued the melanin content, pigmentation gene expression, and the γ -H2AX phosphorylation level in si*Med23* cells (Figures 4D–4F). Furthermore, the expression levels of several DNA repair genes that were altered by *Med23* knockdown could be reversed, at least partially, by ectopic *Mitf* expression (Figure 4G). These results suggest that MITF is a key downstream effector of MED23 in regulating pigmentation and DNA repair.

We next investigated the function of MITF in pigmentation and DNA repair in melanoma cells. Control and albinotic *Mitf*-depleted cells were subjected to UVR, followed by different incubation periods. The loss of *Mitf* resulted in clearly less DNA damage accumulation and elevated NER protein expression, similar to *Med23*-deficient cells (Figure 4H). Chromatin isolation assays revealed that NER proteins were more strongly recruited to chromatin in *Mitf*-depleted melanoma cells, both basally and following UVR (Figure 4I). Using qRT-PCR, we characterized the expression levels of different sets of pigmentation and DNA repair genes that were previously shown to be important for both pathways. Consistent with the results following *Med23* depletion, the pigmentation genes were collectively downregulated, and several DNA repair genes were strongly upregulated (with a minor difference regarding the effect of *Med23* KD) (Figure 4J). In summary, we found that MED23 and MITF both act positively in pigmentation regulation and negatively in DNA repair regulation. Therefore, MITF, as a downstream effector of MED23, appears to phenocopy MED23 in both processes, suggesting the existence of a MED23-MITF axis as the molecular link between pigmentation and DNA damage response.

MED23 Controls *Mitf* Expression by Modulating Its Enhancer Function

We next investigated how MED23 regulates *Mitf*. To this end, we have performed multiple experiments including chromatin immunoprecipitation (ChIP), promoter analysis, and luciferase reporter assays, and have excluded the possibilities that

MED23 act as a cofactor for MITF or regulates its proximal promoter activity. We then performed a ChIP sequencing (ChIP-seq) analysis to explore genomic regulation. First, we analyzed the genome-wide binding profile of Pol II and found minimal differences in global Pol II binding between control and *Med23* knockdown cells (Figures S5A and S5B), the same as the H3K27ac profiles. However, guided by the ChIP-seq profile of H3K27ac, certain putative regulatory regions for *Mitf* were identified, including a distal enhancer, a proximal enhancer, and a terminal enhancer (Figure 5A). When examining the *Mitf* locus, we found that the binding peaks of Pol II to its distal, proximal, and terminal enhancer regions were largely reduced in *Med23* knockdown cells (Figures 5A and 5B). A ChIP assay was performed to verify that Pol II occupancy at these *Mitf* enhancer regions was indeed reduced by *Med23* depletion (Figure 5C). Then we cloned each of these regulatory regions into a luciferase reporter plasmid and performed transient transfection assays in control and *Med23*-deficient cells. A reporter driven by the distal putative enhancer showed reporter expression in control cells but was largely inhibited in *Med23*-depleted cells, whereas reporters driven by fragments containing the proximal and terminal enhancers did not show much transcription activity (Figure 5D). These observations suggest that MED23 is likely important for the distal enhancer activity of *Mitf*.

To further validate the MED23-dependent function of this newly identified *Mitf* enhancer, we deleted this enhancer region using two pairs of CRISPR/Cas9 guide RNAs to create double-strand DNA breaks flanking this enhancer region (Figure 5E). Two independent cell clones (D150 and D156) were obtained with the deletion of the endogenous distal enhancer of *Mitf*. Sequencing confirmed that this endogenous distal enhancer of *Mitf* was deleted successfully, and both clones showed significant downregulation of MITF and, consequently, whitened pigment cells (Figure 5F). These results indicate that MED23 controls MITF expression through this distal enhancer region. Collectively, our study characterizes a novel function of the MED23-MITF axis in coupling the pigmentation and DNA repairing processes (Figure 5G), which provides new mechanistic insights into normal skin development and skin-related diseases.

DISCUSSION

In this study, we identified an unexpected role of the Mediator complex in pigmentation and DNA repair. We initially observed that depletion of MED23 caused the normally dark melanoma cells to adopt a pale color, accompanied by decreased tyrosinase activity. The whitening of dark cells is correlated with decreased protection against genomic DNA damage following

(G) qRT-PCR analysis of DNA repair genes in control, si*Med23*, and hMITF-expressed si*Med23* melanoma cells. The expression was normalized to *Gapdh*. Error bars indicate SEM.

(H) Expression of DNA damage response and repair players at different time points after UV radiation. Control and *Mitf*-deficient B16F10 cells were exposed to 70 J/m² UV. After further incubation for the indicated periods of time, the cells were harvested and subjected to immunoblotting analysis of the indicated proteins. γ -TUBULIN was blotted as an internal control.

(I) Chromatin-bound NER factors after UV radiation. Control and *Mitf*-deficient melanoma cells were similarly UV-irradiated, and chromatin was isolated following incubation for different times. NER proteins were immunoblotted using antibodies against XPA and XPC. Histone H2B and GAPDH were loaded as internal controls for chromatin and soluble fractions, respectively.

(J) qRT-PCR analysis of pigmentation genes and DNA repair genes in control and *Mitf*-deficient cells. The expression was normalized to *Gapdh*. Error bars indicate SEM.

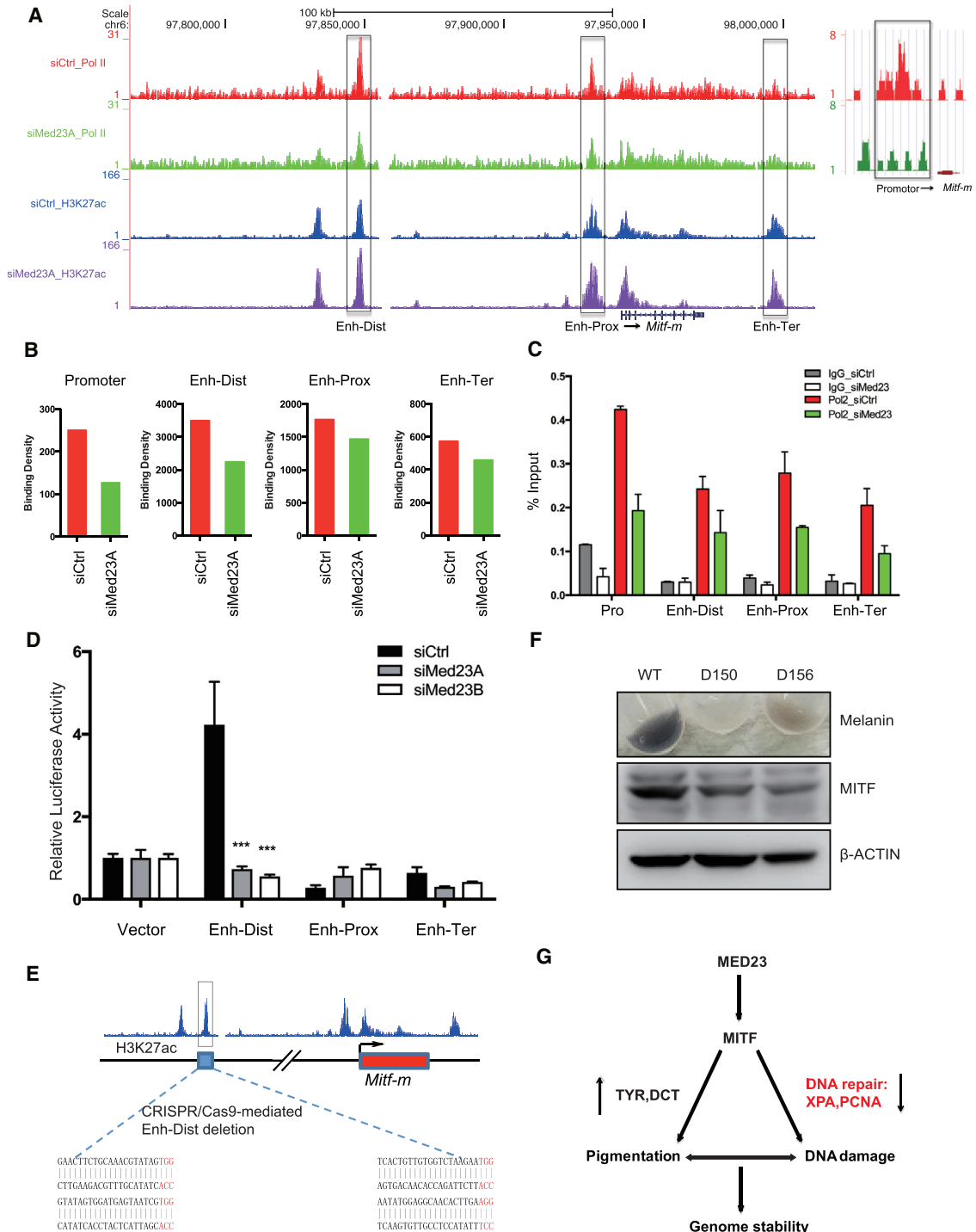


Figure 5. Mediator MED23 Modulates the Activity of a Distal Enhancer of *Mitf*

(A) ChIP-seq analysis of Pol II enrichment at the *Mitf* gene locus in control and *Med23* knockdown melanoma cells. Compared with H3K27ac ChIP-seq data, some putative enhancer regions of *Mitf* were predicted as shown.

(B) Relative quantification of the indicated peaks shown in (A).

(C) Verification of the ChIP analysis at the *Mitf* locus indicated in (A). ChIP assays were performed with an antibody specific for Pol II in control and *Med23*-deficient melanoma cells. Error bars indicate SEM.

(D) Putative enhancer reporter assay. Enhancer activity was measured by the ratio of firefly luciferase activity over *Renilla* luciferase activity (Firefly/*Renilla*) and normalized to the empty vector control. Data are mean ± SEM of three independent experiments.

(legend continued on next page)

extrinsic stress, such as UVR. Moreover, the NER factors were upregulated and enriched at chromatin during UV-induced DNA damage response and repair in *Med23*-deficient cells. Importantly, the transcription-coupled NER seemed not to be involved here because we observed that UV treatment greatly reduced global Pol II binding in both control and si*Med23* melanoma cells (Figures S5C–S5E), suggesting global transcriptional repression. Thus, the loss of *Med23* contributes to enhanced UV-induced NER by increasing NER factor abundance and efficiency.

These findings reveal that melanocytes may adaptively increase their DNA repair capacity after the loss of pigmentation as a form of resistance against genotoxic stress. It is known that cell fate changes (i.e., a tendency toward gaining stemness) could drive enhanced DNA repair capacity and increase genomic stability (Tichy and Stambrook, 2008; Xiong et al., 2015). In our study, decreased pigmentation correlated with a tendency toward cell dedifferentiation and enhanced DNA repair ability, as indicated by the downregulation of melanocyte differentiation genes and increases in the cell growth rate and growth signaling pathways (MAPK pathway) (Figures S1E and S1F) as well as NER enhancement. Generally, in *Med23*-deficient cells, impaired pigmentation offers less protection to genomic DNA; therefore, the cells may exhibit increased NER capacity as a means to better counteract UV-induced photolesions. We therefore propose that *Med23* deficiencies may induce melanocyte dedifferentiation and confer better genomic stability.

Extensive studies have shown that DNA damage itself is important for triggering pigment production and that melanin synthesis may be part of this DNA damage response system (Eller et al., 1994; Gilchrist et al., 1993). Our study reveals that the Mediator complex subunit MED23 is a novel regulator of mammalian melanocytes that inversely coordinates pigmentation and DNA repair, particularly UV-induced NER. The identification of this MED23-MITF molecular axis provides new insights into the cutaneous response to UVR and related skin malignancies.

EXPERIMENTAL PROCEDURES

Cells and Cell Culture

B16F10, A375, and B16 cells were from the type culture collection of the Chinese Academy of Sciences. *Med23*^{+/+} and *Med23*^{-/-} MEFs were generated as described previously (Wang et al., 2009). Clone M3 and primary epidermal melanocytes were from the ATCC. See the [Supplemental Experimental Procedures](#) for details.

Western Blot Analysis and Real-Time PCR

Real-time PCR and western blot analysis were performed as described previously (Yao et al., 2015). See the [Supplemental Experimental Procedures](#) for details.

Retrovirus Infection

Use of a retrovirus to establish stable cell lines for knocking down or overexpressing a gene of interest was based on the manufacturer's recommendations (Clontech). See the [Supplemental Experimental Procedures](#) for details.

RNA-Seq and Data Analysis

Total RNAs were extracted by TRIZOL (Invitrogen) and purified by the QIAGEN RNeasy kit. DNA library preparation and sequencing were performed following the Illumina standard protocol. GO analysis was performed by the Database for Annotation, Visualization, and Integrated Discovery (DAVID) online tool.

Melanin Content

For melanin content determination, cells (5×10^6) were solubilized in 1 N NaOH containing 10% DMSO at 100°C for 30 min. The absorbance at 450 nm was measured using a spectrophotometer (Thermo Multiscan MK3).

Tyrosinase Activity

Tyrosinase enzyme activity was analyzed by measuring the rate of L-DOPA oxidation. In brief, cells (5×10^6) were harvested and lysed in 0.1 M NaH₂PO₄ containing protein inhibitor. Cell extracts were centrifuged at $13,000 \times g$ for 15 min at 4°C, and the supernatants were incubated with 0.1% L-DOPA prepared in 0.1 M NaH₂PO₄ at 37°C for 2 hrs. The absorbance was measured at 450 nm using a spectrophotometer (Thermo Multiscan MK3).

Zebrafish

Two MOs blocking MED23 translation and a control (Ctrl) MO were designed against the 5'-terminal sequence near the start codon and were purchased from Gene Tools. The microinjection was performed in one- to two-cell-stage embryos. See [Table S1](#) for the MO sequences.

Luciferase Assay

A dual luciferase reporter assay was performed using the Dual-Luciferase Reporter Assay System (Promega). See the [Supplemental Experimental Procedures](#) for details.

ChIP, ChIP-Seq, and Data Analysis

ChIP assays were performed as described previously (Huang et al., 2012; Wang et al., 2009; Yao et al., 2015). See the [Supplemental Experimental Procedures](#) for details.

TEM

For TEM studies, ultrathin sections (80 nm) were cut on an RMC Ultramicrotome, placed on copper grids, stained with uranyl acetate and lead citrate, and examined on a JEM 2100F transmission electron microscope.

Chromatin Isolation

Chromatin was fractionated as described previously (Huang et al., 2012). Cells were harvested and suspended in buffer A (10 mM 4-(2-hydroxyethyl)-1-piperazineethanesulfonic acid [HEPES] [pH 7.9], 10 mM KCl, 1.5 mM MgCl₂, 0.34 M sucrose, 10% glycerol, and 0.1% Triton X-100) for 5 min and then in buffer B (10 mM HEPES [pH 7.9] and 10 mM EDTA) for 30 min. The supernatant contained both cytoplasmic and nucleoplasmic fractions. The loading buffer was then added directly to the pellet to make the chromatin fraction.

Immunofluorescence Staining

The immunofluorescence staining assay was performed as described previously (Huang et al., 2012). See the [Supplemental Experimental Procedures](#) for details.

Comet Assay

The comet assay was performed using the comet assay kit from Cell Biolabs according to the manufacturer's instructions. See the [Supplemental Experimental Procedures](#) for details.

(E) Design of CRISPR/Cas9-mediated deletion of the *Mitf* distal enhancer. Sequences for sgRNAs are displayed for protospacer-adjacent motifs (PAMs) highlighted in red.

(F) The cell pellet and MITF protein level of two clones, D150 and D156, that are depleted of the *Mitf* distal enhancer.

(G) A schematic model for Mediator MED23 in regulating pigmentation and DNA repair.

CRISPR/Cas9-Mediated Genomic Engineering

The CRISPR/Cas9 system was applied to introduce the distal enhancer of the *Mitf* deletion mutation following published protocols (Cong et al., 2013; Mali et al., 2013). See the Supplemental Experimental Procedures for details.

ACCESSION NUMBERS

The accession numbers for the RNA-seq data and ChIP-seq data reported in this paper are GEO: GSE98607 and GSE98606.

SUPPLEMENTAL INFORMATION

Supplemental Information includes Supplemental Experimental Procedures, five figures, and one table and can be found with this article online at <http://dx.doi.org/10.1016/j.celrep.2017.07.056>.

AUTHOR CONTRIBUTIONS

M.X. and G.W. designed the project. M.X. performed most experiments. K.C. performed most experiments during revision. X.Y., Y.X., J. Yao, J. Yan, and Z.S. performed the bioinformatic analysis. M.X., K.C., and G.W. wrote the manuscript.

ACKNOWLEDGMENTS

We thank Drs. Guanghui Liu (Institute of Biophysics, Beijing) and Ting Chen (National Institute of Biological Science, Beijing) for their comments and suggestions. This study was supported in part by grants from the Chinese Academy of Sciences (XDB19020100) and the Ministry of Science and Technology of China (2017YFA0102701 and 2014CB964702).

Received: March 28, 2016

Revised: April 8, 2017

Accepted: July 19, 2017

Published: August 22, 2017

REFERENCES

- Bertolotto, C., Abbe, P., Hemesath, T.J., Bille, K., Fisher, D.E., Ortonne, J.P., and Ballotti, R. (1998). Microphthalmia gene product as a signal transducer in cAMP-induced differentiation of melanocytes. *J. Cell Biol.* **142**, 827–835.
- Budden, T., and Bowden, N.A. (2013). The role of altered nucleotide excision repair and UVB-induced DNA damage in melanomagenesis. *Int. J. Mol. Sci.* **14**, 1132–1151.
- Compe, E., and Egly, J.M. (2012). TFIIH: when transcription met DNA repair. *Nat. Rev. Mol. Cell Biol.* **13**, 343–354.
- Cong, L., Ran, F.A., Cox, D., Lin, S., Barretto, R., Habib, N., Hsu, P.D., Wu, X., Jiang, W., Marraffini, L.A., and Zhang, F. (2013). Multiplex genome engineering using CRISPR/Cas systems. *Science* **339**, 819–823.
- DiGiovanna, J.J., and Kraemer, K.H. (2012). Shining a light on xeroderma pigmentosum. *J. Invest. Dermatol.* **132**, 785–796.
- Eller, M.S., Yaar, M., and Gilchrist, B.A. (1994). DNA damage and melanogenesis. *Nature* **372**, 413–414.
- Garibyan, L., and Fisher, D.E. (2010). How sunlight causes melanoma. *Curr. Oncol. Rep.* **12**, 319–326.
- Gilchrist, B.A., Zhai, S., Eller, M.S., Yarosh, D.B., and Yaar, M. (1993). Treatment of human melanocytes and S91 melanoma cells with the DNA repair enzyme T4 endonuclease V enhances melanogenesis after ultraviolet irradiation. *J. Invest. Dermatol.* **101**, 666–672.
- Goding, C.R. (2000). *Mitf* from neural crest to melanoma: signal transduction and transcription in the melanocyte lineage. *Genes Dev.* **14**, 1712–1728.
- Hanawalt, P.C., and Spivak, G. (2008). Transcription-coupled DNA repair: two decades of progress and surprises. *Nat. Rev. Mol. Cell Biol.* **9**, 958–970.
- Hodis, E., Watson, I.R., Kryukov, G.V., Arold, S.T., Imielinski, M., Theurillat, J.P., Nickerson, E., Auclair, D., Li, L., Place, C., et al. (2012). A landscape of driver mutations in melanoma. *Cell* **150**, 251–263.
- Hoek, K.S., Schlegel, N.C., Eichhoff, O.M., Widmer, D.S., Praetorius, C., Einarsson, S.O., Valgeirsdottir, S., Bergsteinsdottir, K., Schepsky, A., Dummer, R., and Steingrímsson, E. (2008). Novel MITF targets identified using a two-step DNA microarray strategy. *Pigment Cell Melanoma Res.* **21**, 665–676.
- Huang, Y., Li, W., Yao, X., Lin, Q.J., Yin, J.W., Liang, Y., Heiner, M., Tian, B., Hui, J., and Wang, G. (2012). Mediator complex regulates alternative mRNA processing via the MED23 subunit. *Mol. Cell* **45**, 459–469.
- Kang, Y.K., Guermah, M., Yuan, C.X., and Roeder, R.G. (2002). The TRAP/Mediator coactivator complex interacts directly with estrogen receptors alpha and beta through the TRAP220 subunit and directly enhances estrogen receptor function in vitro. *Proc. Natl. Acad. Sci. USA* **99**, 2642–2647.
- Karahalil, B., Bohr, V.A., and Wilson, D.M., 3rd. (2012). Impact of DNA polymorphisms in key DNA base excision repair proteins on cancer risk. *Hum. Exp. Toxicol.* **31**, 981–1005.
- Kim, S., Xu, X., Hecht, A., and Boyer, T.G. (2006). Mediator is a transducer of Wnt/beta-catenin signaling. *J. Biol. Chem.* **281**, 14066–14075.
- Kimmel, C.B., Ballard, W.W., Kimmel, S.R., Ullmann, B., and Schilling, T.F. (1995). Stages of embryonic development of the zebrafish. *Dev. Dyn.* **203**, 253–310.
- Kraemer, K.H., Patronas, N.J., Schiffmann, R., Brooks, B.P., Tamura, D., and DiGiovanna, J.J. (2007). Xeroderma pigmentosum, trichothiodystrophy and Cockayne syndrome: a complex genotype-phenotype relationship. *Neuroscience* **145**, 1388–1396.
- Lehmann, A.R., McGibbon, D., and Stefanini, M. (2011). Xeroderma pigmentosum. *Orphanet J. Rare Dis.* **6**, 70.
- Lin, J.Y., and Fisher, D.E. (2007). Melanocyte biology and skin pigmentation. *Nature* **445**, 843–850.
- Mali, P., Yang, L., Esvelt, K.M., Aach, J., Guell, M., DiCarlo, J.E., Norville, J.E., and Church, G.M. (2013). RNA-guided human genome engineering via Cas9. *Science* **339**, 823–826.
- Malik, S., and Roeder, R.G. (2010). The metazoan Mediator co-activator complex as an integrative hub for transcriptional regulation. *Nat. Rev. Genet.* **11**, 761–772.
- Steingrímsson, E., Copeland, N.G., and Jenkins, N.A. (2004). Melanocytes and the microphthalmia transcription factor network. *Annu. Rev. Genet.* **38**, 365–411.
- Stevens, J.L., Cantin, G.T., Wang, G., Shevchenko, A., and Berk, A.J. (2002). Transcription control by E1A and MAP kinase pathway via Sur2 mediator subunit. *Science* **296**, 755–758.
- Strub, T., Giuliano, S., Ye, T., Bonet, C., Keime, C., Kobi, D., Le Gras, S., Cormont, M., Ballotti, R., Bertolotto, C., and Davidson, I. (2011). Essential role of microphthalmia transcription factor for DNA replication, mitosis and genomic stability in melanoma. *Oncogene* **30**, 2319–2332.
- Tichy, E.D., and Stambrook, P.J. (2008). DNA repair in murine embryonic stem cells and differentiated cells. *Exp. Cell Res.* **314**, 1929–1936.
- Wang, W., Huang, L., Huang, Y., Yin, J.W., Berk, A.J., Friedman, J.M., and Wang, G. (2009). Mediator MED23 links insulin signaling to the adipogenesis transcription cascade. *Dev. Cell* **16**, 764–771.
- Xiong, J., Todorova, D., Su, N.Y., Kim, J., Lee, P.J., Shen, Z., Briggs, S.P., and Xu, Y. (2015). Stemness factor Sall4 is required for DNA damage response in embryonic stem cells. *J. Cell Biol.* **208**, 513–520.
- Yang, X., Zhao, M., Xia, M., Liu, Y., Yan, J., Ji, H., and Wang, G. (2012). Selective requirement for Mediator MED23 in Ras-active lung cancer. *Proc. Natl. Acad. Sci. USA* **109**, E2813–E2822.
- Yao, X., Tang, Z., Fu, X., Yin, J., Liang, Y., Li, C., Li, H., Tian, Q., Roeder, R.G., and Wang, G. (2015). The Mediator subunit MED23 couples H2B mono-

ubiquitination to transcriptional control and cell fate determination. *EMBO J.* 34, 2885–2902.

Yin, J.W., Liang, Y., Park, J.Y., Chen, D., Yao, X., Xiao, Q., Liu, Z., Jiang, B., Fu, Y., Bao, M., et al. (2012). Mediator MED23 plays opposing roles in directing smooth muscle cell and adipocyte differentiation. *Genes Dev.* 26, 2192–2205.

Yin, J.W., and Wang, G. (2014). The Mediator complex: a master coordinator of transcription and cell lineage development. *Development* 141, 977–987.

Zhu, W., Yao, X., Liang, Y., Liang, D., Song, L., Jing, N., Li, J., and Wang, G. (2015). Mediator Med23 deficiency enhances neural differentiation of murine embryonic stem cells through modulating BMP signaling. *Development* 142, 465–476.